Nanodosimetry-based quality factors for radiation protection in space

Reinhard W. Schulte[1,2,*], Andrew J. Wroe[2], Vladimir A. Bashkirov[2], Guy Y. Garty[3], Amos Breskin[4], Rachel Chechik[4], Sergei Shchemelinin[4], Elisabetta Gargioni[5], Bernd Grosswendt[5], Anatoly B. Rosenfeld[6]

[1] Department of Radiation Medicine, Loma Linda University Medical Center, B121, 11234 Anderson Street, Loma Linda, CA 92354, USA
[2] Department of Radiation Medicine, Loma Linda University Medical Center, Loma Linda, CA 92354, USA
[3] RARAF, Columbia University, P.O. Box 21, Irvington, NY 10533, USA
[4] Department of Particle Physics, Weizmann Institute of Science, Rehovot, 76100, Israel
[5] Physikalisch-Technische Bundesanstalt (PTB), Braunschweig, D-38116, Germany
[6] Centre for Medical Radiation Physics, University of Wollongong, Wollongong, NSW 2087, Australia

Received 2 January 2008; accepted 26 June 2008

Abstract

Evaluation and monitoring of the cancer risk from space radiation exposure is a crucial requirement for the success of long-term space missions. One important task in the risk calculation is to properly weigh the various components of space radiation dose according to their assumed contribution to the cancer risk relative to the risk associated with radiation of low ionization density. Currently, quality factors of radiation both on the ground and in space are defined by national and international commissions based on existing radiobiological data and presumed knowledge of the ionization density distribution of the radiation field at a given point of interest. This approach makes the determination of the average quality factor of a given radiation field a rather complex task. In this contribution, we investigate the possibility to define quality factors of space radiation exposure based on nanodosimetric data. The underlying formalism of the determination of quality factors on the basis of nanodosimetric data is described, and quality factors for protons and ions (helium and carbon) of different energies based on simulated nanodosimetric data are presented. The value and limitations of this approach are discussed.

Bewertungsfaktoren für den Strahlenschutz im Weltraum basierend auf nanodosimetrischen Daten

Zusammenfassung

Abschätzung und Überwachung des Krebsrisikos durch Strahlungsbelastung im Weltraum ist eine wichtige Voraussetzung für den Erfolg von Langzeit-Missionen im Weltraum. Eine wichtige Aufgabe für die Risikoabschätzung ist die adäquate Gewichtung des Beitrages der verschiedenen Komponenten der kosmischen Strahlung zu dem Krebsrisiko relativ zur Strahlung niedriger Ionisationsdichte. Derzeit werden Bewertungsfaktoren der terrestrischen und extraterrestrischen Strahlung durch nationale und internationale Kommissionen festgelegt, basierend auf dem aktuellen strahlenbiologischen Kenntnisstand und der angenommenen Verteilung der Ionisationsdichte der Strahlung am jeweiligen Bewertungsort. Dieser Ansatz macht die Bestimmung von Bewertungsfaktoren für die Strahlung im Weltraum relativ kompliziert. In diesem Beitrag berichten wir über die Möglichkeit, Bewertungsfaktoren für den Strahlenschutz im Weltraum mit Hilfe von nanodosimetrischen Daten zu bestimmen. Der zugrunde gelegene Formalismus wird beschrieben, und Bewertungsfaktoren für Protonen und Ionen (Helium und Kohlenstoff) basierend

* Corresponding author. Department of Radiation Medicine, Loma Linda University Medical Center, B121, 11234 Anderson Street, Loma Linda, CA 92354, USA. Tel.: 001-909-558-4243.

E-mail: rschulte@dominion.llumc.edu (R.W. Schulte).

Keywords: nanodosimetry, space radiation, quality factors

auf nanodosimetrischen Daten werden vorgestellt. Vorteil und Grenzen dieser Methode werden diskutiert.

Schlüsselwörter: Nanodosimetrie, kosmische Strahlung, Bewertungsfaktoren

Introduction

The risk of radiation-induced cancer and other late radiation effects from exposure to space radiation is one of the major challenges of long-term space exploration; humans will be exposed to these hazardous radiation fields for longer periods of time than has ever been experienced. Space radiation comprises a wide range of particles with a broad spectrum of energies. For example, the space radiation environment in low earth orbit (LEO) contains galactic cosmic rays (GCR) and energetic solar particles, i.e., electrons and protons, as well as neutrons and photons generated by inelastic nuclear interactions in the Earth's atmosphere and in the spacecraft's hull. Beyond the Earth's magnetic field, the radiation environment is dominated by GCR superimposed with relatively short solar particle events (SPEs) associated with coronal mass ejections. In the energy range from 100 MeV per nucleon to 10 GeV per nucleon, GCR consist of 87 percent protons, 12 percent helium ions, and 1 percent heavier ions [1]. Due to their high energy, GCR easily penetrate the shielding of spacecraft and a variety of secondary charged particles and neutrons is produced. Protons are also the major component of SPEs, which, due to their high fluence rates, pose an acute risk for the health of astronauts.

Close monitoring of the radiation exposure of humans in outer space and on the surface of landing sites not only requires measurement of the absorbed dose received by personnel but also assessment of the radiation quality. For the evaluation of space radiation exposure, the lifetime fatal cancer risk is estimated by multiplying an age- and gender-dependent risk coefficient and the dose equivalent, which is generally defined as the product of absorbed dose, D, and the quality factor, Q, associated with the radiation environment. In the United States, the National Council on Radiation Protection (NCRP) has adopted the organ dose equivalent, H_T, as the appropriate quantity for radiation protection in space [2]. This quantity, which was defined by the International Commission on Radiation Units (ICRU) [3], is given by

$$H_T = \frac{1}{m_T}\int_{m_T}\left(\int_L Q(L)D(L)\mathrm{d}L\right)\mathrm{d}m \qquad (1)$$

where $Q(L)$ is the quality factor as a function of linear energy transfer (LET), L, previously defined by the International Commission on Radiological Protection (ICRP) [4], $D(L)\mathrm{d}L\mathrm{d}m$ is the dose deposited in the mass element $\mathrm{d}m$ by radiation in the LET range between L and $L+\mathrm{d}L$, and the integration is over the entire LET range observed and over the mass of the organ.

Organ dose equivalents for representative SPEs and annual GCR spectra have been determined using radiation transport codes such as BRYNTRN and HZETRN [5] in combination with computerized human anatomical models [6]. Although this approach provides useful estimates of the radiation dose and cancer risk in space, there are disadvantages including uncertainties of the radiation transport codes and difficulties with LET as a unique descriptor of radiation quality. Alternative methodologies including a fluence-based approach and a microdosimetric event-based approach have been suggested to overcome some of these problems [7].

In this contribution, we present a new approach that defines quality factors based on nanodosimetric ionization cluster-size distributions. Nanodosimetry is a relatively new technique that measures the number of ions induced by charged particles within a wall-less sensitive gas volume representing a DNA segment [8]. Since radiation carcinogenesis is believed to be initiated by a DNA damaging event, one can assume that the risk of cancer induction is proportional to the number of such initiating events. Direct measurements of the number of radiation-induced events involving a complex DNA damage allows calculating a quality factor defined as the ratio of the frequency of such events induced by space radiation to that of low-LET reference radiation. The results of this approach with protons and light ions are presented and its advantages and limitations are discussed.

Methods

Nanodosimetry and the Ion-counting Nanodosimeter

Nanodosimetry provides a means for measuring the number of radiation-induced ionizations within a nanoscopic sensitive volume (SV). With existing technology using a low-pressure gas, the interaction volume is magnified to the millimeter scale and, therefore, accessible to direct measurement. The quantity of interest for applications in radiation protection is the frequency distribution of ionization clusters formed in a SV that simulates ionizations in a DNA-like segment and the surrounding water layer,

from which radiation-induced radicals can diffuse to the DNA and damage it.

The nanodosimeter developed at the Weizmann Institute of Science and Loma Linda University is shown schematically in Figure 1. The interaction volume of the device is a cylindrical gas volume of 120 Pa propane, 5 cm in height and 5 cm in diameter. The scaling condition is: 1 mm in the detector corresponds to 2.8 nm in water.

A wall-less, narrow and elongated SV is formed by means of superposition of electric fields E_1 and E_2. The radiation-induced positive ions drift toward a 1-mm diameter aperture at the bottom of the gas volume under electric field E_1 of 60 V/cm. The electric field E_2 extracts the ions through the aperture and accelerates them toward a vacuum-operated ion-counting electron multiplier (model AF180HIG, SGE Analytical Science, Melbourne, Australia); ions are accelerated through a potential difference of 8 kV with respect to the aperture plate. For a single primary particle, a cluster of radiation-induced ions in the SV results in a train of pulses that is registered by the nanodosimeter data acquisition system; the trigger is provided by the primary particle traversing the gas volume [9,10] (Fig. 2a). The SV is defined by the three-dimensional distribution of ion collection efficiency (Fig. 2b), which has been both measured and calculated using a Monte Carlo ion transport code with good agreement of both data sets [11]. The ion origin along the SV is derived from its drift-time measurement; selection of certain drift-time limits permits segmenting the full-length SV into shorter sub-volumes [9,10]. Selectable tissue-equivalent SV lengths range from about 5 nm, which is the resolution limit due to ion diffusion, to about 150 nm, which is the maximum length defined by the height of the gas volume. A more detailed description of the nanodosimeter (ND) and its performance has been given elsewhere [9,10].

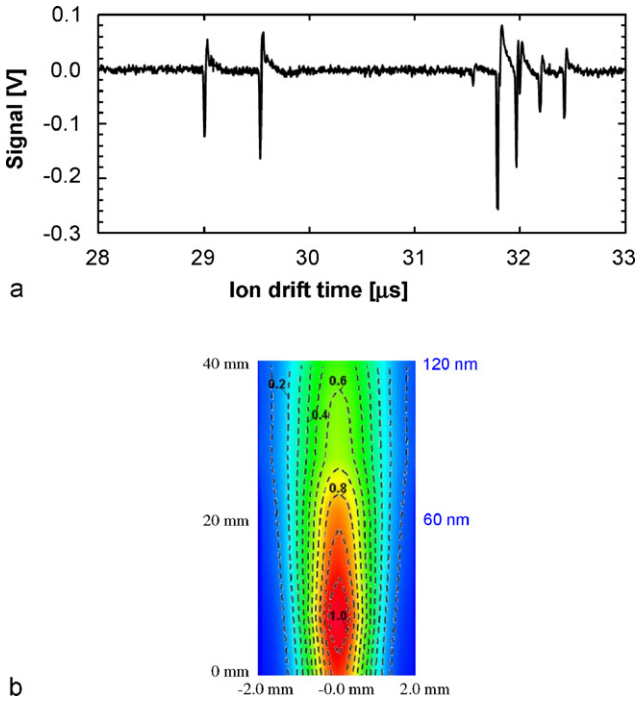

Figure 2. (a) Sequence of electrical signals registered from the ion counter, each pulse corresponds to a single ion induced by one primary charged particle. (b) Efficiency map of the sensitive volume.

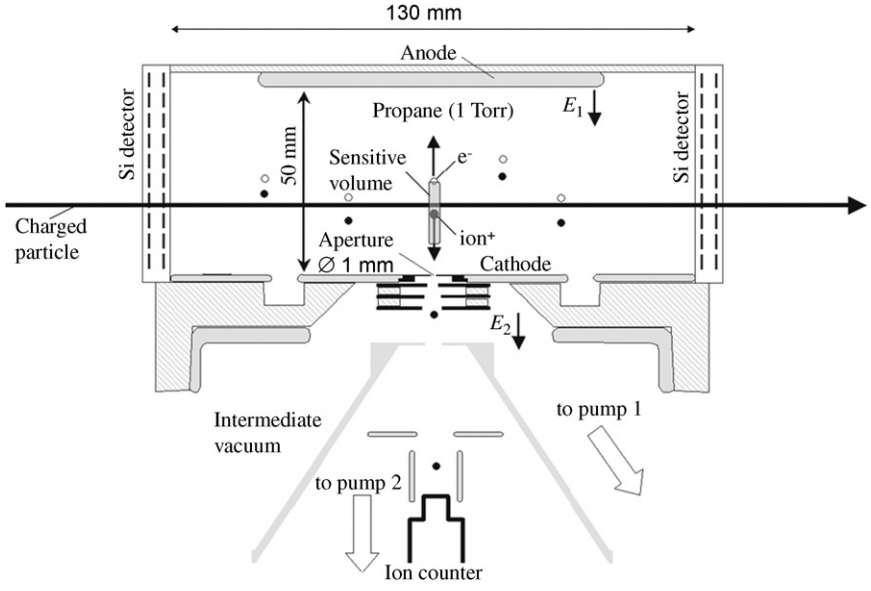

Figure 1. Cross-sectional view of the nanodosimeter installed on the proton research beam line at Loma Linda University Medical Center.

It is important to note that the SV was conceptually designed to simulate a cylindrical segment of DNA with the surrounding water shell of a few nanometers in thickness from which damaging species produced in water radiolysis can diffuse to the DNA. With the current configuration of the SV ion extraction efficiency (Fig. 2b), it is reasonable to assume that we are approximately simulating the high efficiency of direct DNA ionizations within a cylinder of about 2 nm diameter (0.8 mm in the ND gas phase) matching that of the DNA double helix, whereas the rapidly falling ion collection efficiency with radial distance from the SV axis simulates the efficiency of diffusing water radicals and hydrated electrons to cause damage in the DNA.

Monte Carlo Simulation of Nanodosimetric Data

In this work, we simulated nanodosimetric cluster-size distributions of electrons, protons, and light ions with a dedicated Monte Carlo code developed at PTB and described in detail in [10,12]. The code, in its current form, utilizes a cubic propane gas volume of 125 cm^3 and a combination of experimental and theoretical ionization cross sections of electrons, protons and light ions up to neon; it simulates the transport of charged hadrons and electrons in the gas with energies down to 10 eV (e.g., the ionization potential of propane). The code calculates the location of the ions induced by the primary particle in the SV, which is defined by a look-up table of ion collection efficiencies as a function of radial distance from the SV axis and height above aperture plane. Ion clusters are then transformed into ion-signal pulse trains based on the experimentally measured location-vs.-drift time relationship. The code has been benchmarked against experimental data with good agreement [10,13–15].

Track segments of low-LET 100-keV electrons (0.4 keV/μm) and charged hadrons, including protons, helium-4 ions, and carbon-12 ions with LET values ranging from 0.4 to approximately 800 keV/μm were simulated. LET values in water were taken from SRIM [16] (Table 1). Ions were assumed to be in a fixed charge state given by their equilibrium mean charge. Particle energies were selected to provide an overlap in LET values between the different hadrons. Electrons were chosen as the low-LET reference radiation. The primary particles were incident on the gas volume perpendicular to the SV axis as a uniform circular beam of 3 cm in diameter. Three different SV sizes were simulated: the full SV without any restrictions, corresponding to about 150 nm on the equivalent nanometer scale, a 16 nm-equivalent long SV (about 50 base pairs on the DNA scale), and a 7 nm-equivalent long SV (about 20 base pairs). All simulations were performed with 10^6–10^7 incident primary particles ensuring adequate statistics.

Table 1
Specifications of particles for which nanodosimetric data were simulated in this work.

Particle type	Particle energy (MeV)	Particle LET (keV/μm)
Electron	0.1	0.4
Proton	0.5	40.0
	1.0	25.0
	5.1	8.1
	10	4.7
	20	2.7
	100	0.7
	250	0.4
Helium ion	1	223
	5	91
	10	56
	15	41
	20	33
	25	27
	30	24
Carbon ion	10	797
	20	580
	40	385
	100	202
	250	90

Determination of Quality Factors from Nanodosimetric Data

In order to derive a quality factor for a given radiation, we applied the general model formalism developed and initially validated by Garty [17]. It converts ionization cluster frequencies measured with the nanodosimeter into DNA damage cluster frequencies.

The formalism predicts the probability that a cluster of n_{ion} ions registered in the full or sub-segmented SV of the nanodosimeter produces a DNA damage cluster of a specified number of DNA strand breaks. This probability is then converted into DNA strand break cluster yield, which is defined in the radiochemical sense as number of clusters per unit energy deposited. The model for conversion of ionization cluster size frequencies to DNA strand break clusters has one basic parameter, i.e., the probability, p_{sb}, that an ionization observed in the SV will be converted into a strand break in the equivalent DNA segment.

We have previously estimated the parameter p_{sb} using a least-square fit of double strand break (DSB) yields predicted by the ND-data-based formalism to those obtained with a plasmid DNA assay and found that best-fitting values are in the range of 10–20 percent [17]. This is in agreement with findings from radiochemical studies showing that OH-radicals created from ionizations near the DNA have a probability of about 13 percent to form a DNA strand break and that 65–50 percent of all strand

breaks are due to the indirect effect from diffusing OH radicals, a percentage that is decreasing with increasing LET [18]. In this work, we used a nominal value of $p_{sb} = 0.15$ but also tested the sensitivity of the quality factors with respect to choosing parameter values of 0.10 and 0.20, respectively. To simplify matters, it was assumed that p_{sb} does not depend on LET of the primary radiation.

DSBs are considered important lesions for radiobiological endpoints including cell lethality and cancer induction. Most DSBs are repaired by repair-competent mammalian cells, but complex DSBs, which are associated with additional strand breaks in the vicinity of two opposing strand breaks, pose a problem to the enzymatic repair machinery and often lead to mis-repair since they require the homologous recombination repair mechanism, which is only available in late S and G_2 phases of the cell cycle. Therefore, we assumed that the critical lesions relevant for radiation carcinogenesis are DNA damage clusters with $n_{sb} \geq 3$ and not all strand breaks are located on the same strand.

Assuming that one ion in the nanodosimeter SV corresponds to either none or one strand break in the equivalent DNA segment, the conditional probability to observe a DNA damage cluster with exactly n_{sb} strand breaks given that an ionization cluster with n_{ion} was observed can be described by the binomial probability

$$P_{sb}(n_{sb}|n_{ion}) = \binom{n_{ion}}{n_{sb}} p_{sb}^{n_{sb}} \left(1 - p_{sb}\right)^{n_{ion}-n_{sb}} \tag{2}$$

Let $f_{ND}(n_{ion})$ be a representative nanodosimetric cluster-size distribution, i.e., the relative frequency of events with ionization clusters containing n_{ion} ions obtained with a particular radiation field. The frequency distribution is normalized to the total number of events with one or more ions ($n_{ion} \geq 1$). The frequency of ionization events leading to exactly n_{sb} strand breaks in the DNA segment is then

$$f_{sb}(n_{sb}) = \sum_{n_{ion}=1}^{n_{ion\_max}} f_{ND}(n_{ion}) P_{sb}(n_{sb}|n_{ion}) \tag{3}$$

where n_{ion_max} is the practically observed largest ionization cluster size. Further, let $p_{dsb}(n_{sb}) = 1 - \frac{1}{2}^{n_{sb}-1}$ be the probability that not all out of n_{sb} strand breaks occur on the same DNA strand; the frequency of DSBs with exactly n_{sb} strand breaks ($n_{sb} \geq 2$) is given by

$$f_{dsb}(n_{sb}) = \sum_{n_{ion}=2}^{n_{ion\_max}} f_{ND}(n_{ion}) P_{sb}(n_{sb}|n_{ion}) p_{dsb}(n_{sb}) \tag{4}$$

Further, the frequency of complex DSBs, i.e., those with $n_{sb} \geq 3$, is given by

$$f_{dsb-c} = \sum_{n_{sb}=3}^{n_{ion\_max}} \sum_{n_{ion}=n_{sb}}^{n_{ion\_max}} f_{ND}(n_{ion}) P_{sb}(n_{sb}|n_{ion}) p_{dsb}(n_{sb}) \tag{5}$$

Normalizing this frequency to the average amount of energy deposited per energy deposition event, we have for the yield of critical DSBs

$$G_{dsb-c} = \frac{f_{dsb-c}}{W \sum_{n_{ion}=1}^{n_{ion\_max}} n_{ion} f_{ND}(n_{ion})} \equiv \frac{f_{dsb-c}}{W M_1} \tag{6}$$

where W is the mean energy required to form an electron-ion pair and M_1 is the first moment of the nanodosimetric distribution, which is equivalent to the mean cluster size of events with $n_{ion} \geq 1$.

The nanodosimetric quality factor for a certain radiation was defined as the ratio of complex DSB yields for the radiation under investigation and a reference radiation:

$$Q_{ND} = \frac{G_{dsb-c}}{G_{dsb-c}^{ref}} \tag{7}$$

Due to weak dependence of nanodosimetric cluster-size distributions on LET in the 0.1–1 keV/μ range, the resulting Q factor should not be sensitive to the choice of reference radiation in this LET range. Here, we chose primary electrons of 0.4 keV/μm as reference radiation.

Results

Ion and DNA Damage Cluster-size distributions

Ionization cluster-size distributions were simulated for electrons (reference radiation), protons, helium ions, and carbon ions of different energies (see Table 1) and for three different sensitive volumes (see above). Results for the 16 nm long SV will be presented first and those for the large and smaller volume will be presented below (Dependence of Quality Factors on Sensitive Volume Length). Figure 3 shows representative ionization cluster-size distributions for the 16 nm long SV for the highest and lowest LET values of each particle type. Note that events with a single ion, although not representing a true cluster, were included in the distributions. The distributions were normalized to the number of registered events with at least one ion, excluding particles traversing the gas volume without ion registration in the SV. Ionization cluster-size frequencies generally declined with increasing size, but for high-LET particles intermediate (3–10 ions) and large ionization clusters (>10 ions) where more frequent and small clusters (1 or 2 ions) less frequent than for low LET radiation. There was no obvious LET threshold for large clusters, as these were also observed with low-LET radiation.

Each ionization cluster-size distribution was converted to a distribution of strand breaks per DSB. The resulting distribution, normalized to the total number of DSBs, is

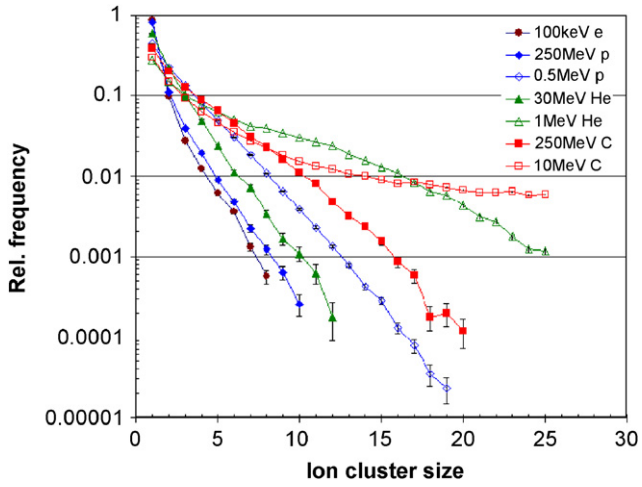

Figure 3. Ionization cluster-size distributions simulated with a sensitive volume of 16 nm equivalent length for the lowest and highest LET of the particle species used in this work.

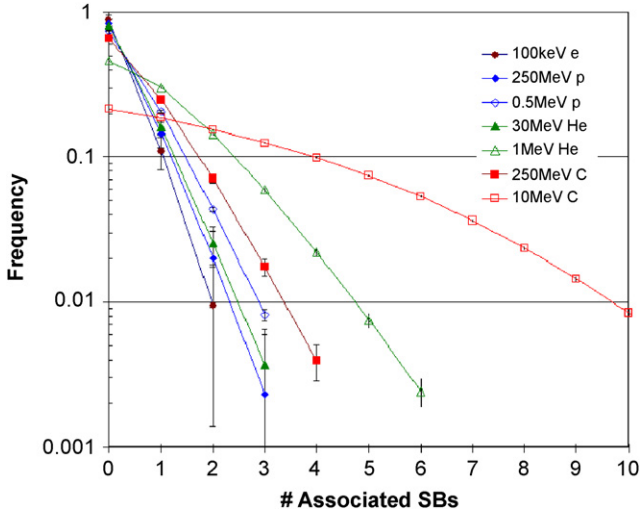

Figure 4. Distribution of the number of strand breaks associated with DSBs based on a conversion of the ionization cluster-size distributions shown in (Fig. 3).

shown in (Fig. 4). DSB complexity was expressed as the number of additional strand breaks associated with a "simple" DSB, defined as two strand breaks on opposing DNA strands within a segment of DNA equivalent to the SV. Thus zero associated strand breaks would correspond to a simple DSB, one associated strand break to a DSB with one additional strand break, etc. It is obvious that for low-LET radiation (100 keV electrons and 250 MeV protons) the majority of DSBs (>80 percent) was simple, whereas for high-LET particles the majority of DSBs was associated with additional strand breaks.

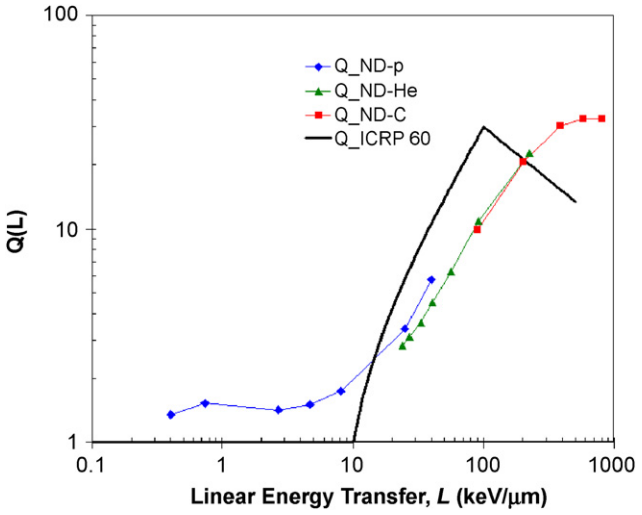

Figure 5. Nanodosimetry-based quality factors as a function of LET derived from ionization cluster-size distributions obtained with a SV of 16 nm equivalent length. The Q-factors from ICRP Publication 60 are shown for comparison.

Quality Factors versus LET

The yield of DSBs with at least three strand breaks (complex DSBs) was derived for each particle type and energy; quality factors were calculated by taking the ratio of this yield to the yield of complex DSBs of 100-keV electrons. The resulting quality factors for the 16 nm long SV are shown in (Fig. 5) as a function of LET and compared to the LET-dependent quality factors defined in ICRP Publication 60 [4]. One should note that the general trend of the quality factors is similar to those defined by the ICRP with practically constant values in the 0.1–10 keV/µm LET range, a steep rise for LET values in the 10–100 keV/µm range, and a leveling-off beyond 100 keV/µm. However, the pronounced quality factor peak at 100 keV/µm, defined by the ICRP, is not seen for the nanodosimetry-based quality factors. Of note, the quality factors for protons with LET values between 0.1 and 10 keV/µm are higher than 1, i.e., about 1.3–1.4, and protons have an about 20 percent higher quality factor than helium ions for the same LET. Differences in quality factors for different particles of the same LET are not defined by the ICRP.

Dependence of Quality Factors on Conversion Probability

We tested the sensitivity of the derived quality factors to the choice of the value of the conversion parameter p_{sb}. Figure 6 shows the quality factor versus LET for the 16 nm long SV for three different values of p_{sb} (0.10,

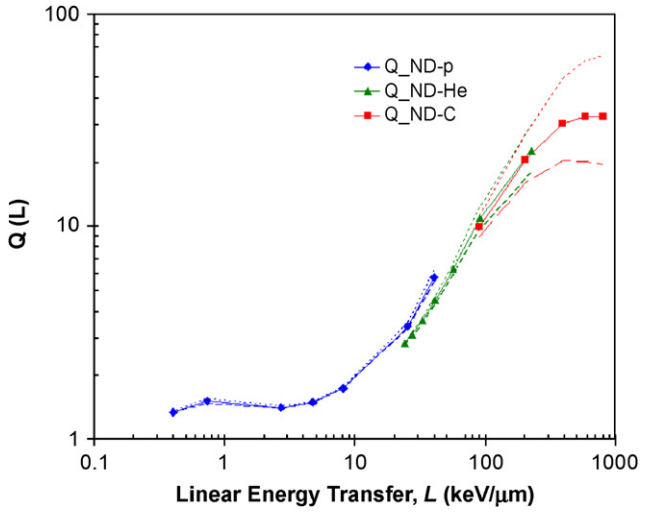

Figure 6. Nanodosimetry-based quality factors as a function of LET derived for different values of the conversion parameter p_{sb}: the upper (dotted) lines connect the values that were calculated with $p_{sb} = 0.10$, the lower (dashed) lines connect the values calculated with $p_{sb} = 0.20$, and the solid lines connect the values calculated with the nominal value of $p_{sb} = 0.15$.

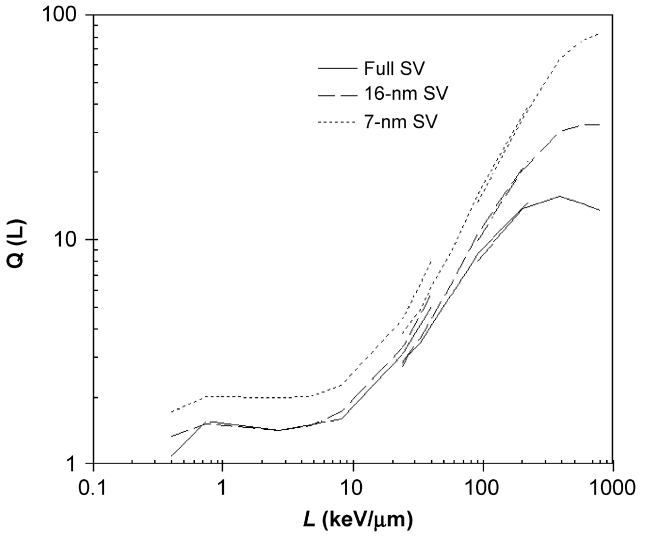

Figure 7. Nanodosimetry-based quality factors as a function of LET for three different sensitive volume sizes.

0.15, and 0.20). The value of $p_{sb} = 0.15$ yielded quality factors closest to those defined in ICRP Publication 60. In the LET range of 0.1–100 keV/µm, the upper and lower limits of quality-factors were within 10 percent of the nominal quality factor values, but larger differences, up to a factor 2.5, were seen for the LET range of 100–1000 keV/µm. Generally, it is obvious that a larger conversion factor will increase the yield of DSBs for any radiation. However, the smaller value ($p_{sb} = 0.10$) resulted in higher quality factors and the higher value ($p_{sb} = 0.20$) in lower quality factors than the intermediate value. This is due to the fact that with increasing p_{sb} the absolute yield of complex DSBs increased more for the low-LET reference radiation than for the radiation of higher LET.

Dependence of Quality Factors on Sensitive Volume Length

We investigated the dependence of quality factors on the length of the sensitive volume (Fig. 7). The 16 nm long SV yielded quality factors that were most compatible with those defined in ICRP Publication 60. The full-length SV, which has an approximate equivalent length of 150 nm, resulted in 2–3 times lower quality factors and the small SV of 7 nm length resulted in about three times higher quality factors. It is clear that the large SV will register many more ionizations including those that may not interact to form DSBs due to a separation larger than the presumed critical distance for interaction (10–20 base pairs or 3–7 nm). This would falsely increase the number of complex DSBs, in particular for low-LET radiation, explaining the lower values for the quality factors derived from the large SV. On the other hand, the small SV (7 nm) is likely to undersample the number of clusters leading to complex DSBs. This may lead to an underestimation of the number of complex DSBs generated by low LET radiation, as the associated ionization clusters are probably spatially less dense than those caused by high-LET radiation. This would explain an overestimation of the quality factor derived from the small SV.

Discussion and Future Directions

Despite current technical limitations preventing compact nanodosimeters to be utilized for space flights, we have investigated the possibility to derive quality factors of space radiation with nanodosimetry. Since experimental data for a larger range of heavy ions and LET values are scarce, we performed Monte Carlo simulations of the experimental nanodosimetric data for protons, helium and carbon ions, as well as 100 keV electrons, the latter used as low-LET reference radiation. The Monte Carlo code developed at the PTB for that purpose has been extensively validated in comparison with experimental nanodosimetric data with protons and helium ions [10,13,14]. For heavier ions, the code remains to be validated as experimental data do not exist at this time.

Our results obtained with a nominal 16 nm long SV and a probability of 0.15 for ion-to-strand-break conversion agree generally well with the $Q(L)$ LET dependence devised by the ICRP in their Publication 60 [4]. One notable

difference in the low-LET range is that the quality factor up to an LET value of 10 keV/μm was in the range of 1.3–1.4 for protons with energies >5 MeV in our work but defined as 1.0 by the ICRP. Our value is consistent with relative biological effectiveness (RBE) values in the range of 1.1–1.2 for high-energy protons compared to γ rays at radiotherapeutic doses (1.8–2 Gy) with a tendency of higher RBEs in the low-dose limit [19]. A second difference is the about 10% higher $Q(L)$ value for protons compared to helium for the same LET This observation is in agreement with higher cell-survival and mutation-induction RBEs of low-energy protons compared to those of helium ions at the same LET [20,21].

It should be mentioned that nanodosimetry is not the only option for evaluating and monitoring quality factors and equivalent doses for space radiation exposure. The use of very compact solid-state microdosimeters to monitor space radiation quality is rapidly evolving and was recently modeled with silicon-on-insulator (SOI) microdosimeters for solar protons [22]. The MIDN (MIcroDosimetry iNstrument) developed by the United States Naval Academy contains three SOI microdosimeters located at three different locations on the MidSTAR-1 spacecraft [23]. MidSTAR-1 is the first of the MidSTAR series and was launched aboard a Lockheed-Martin Atlas V rocket in March 2007. From the microdosimetry spectra recorded by the microdosimeters, the mean dose weighted lineal energy, average quality factor, and dose equivalent can be determined using the protocol outlined in ICRU report 36 [24].

The main difference between the microdosimetry and the nanodosimetry approach to determine quality factors is in the geometry of the sensitive volume and the conversion of event-size distributions into a radiation quality factor. Microdosimetry records stochastic energy deposition events in micrometer volumes and one *assigns* quality factors to components of the lineal energy spectrum. Nanodosimetry, on the other hand, records individual ionizations occurring in simulated DNA segments and one *calculates* the quality factor based on the frequency ratio of critical DNA damage events (complex DSBs). This approach may be more directly related to cancer initiating events, however, additional radiobiological research correlating nanodosimetry data with biological endpoints such as mutations and cancer induction will be needed to confirm this view.

The approach suggested here has its specific limitations, some being of conceptual nature as discussed next, and others of technical nature, as discussed below. There are several assumptions implicit in our approach that should be discussed and critically evaluated.

- Our approach provides quality factors based on the relative frequency of complex DSBs, which are presumably responsible for radiation-induced late effects. Current hazard-rate radiation risk models assume an age-dependent base-line risk modified by a relative risk (RR) factor, which is expressed as the product of a function of the effective dose equivalent and a function of age at exposure and time since exposure [25]. The effective dose equivalent is a weighted sum of organ dose equivalents derived from equation (1) and multiplied with organ-specific weighting factors [26]. The use of a multiplicative quality factor in equation (1), here derived from relative frequency of complex DSBs, implies that the relationship between dose (or fluence) and DSB induction is linear. This is implicit in our model due to the assumption that only single particles contribute to ionization clusters (see last discussion point below), and has also been confirmed by experimental studies of DSB induction [27].
- Central to our approach is the assumption that complex DSBs with three or more strand breaks are the most relevant DNA lesions for radiation-induced cancer. Error-prone repair of DSBs has in fact been recognized as the predominant mechanism for radiation-induced genetic and chromosomal injury leading to cancer in the BEIR VII Phase 2 Committee Report [25]. Moreover, not all DSBs are equal in their reparability and most DSBs with just two breaks separated by a few base pairs can be repaired by the non-homologous end joining (NHEJ) repair mechanism [28]. With any additional break, however, a small piece of DNA or genetic information is lost from the break site and DNA repair appears to become error prone and chromosomal rearrangements are more likely. Moreover, while complex breaks can be repaired in principle by homology-directed repair (HR), this mechanism is not available throughout the cell cycle and has a limited capacity in most mammalian cells [28]. These facts support our assumption that DSBs with three or more strand breaks are relevant in the process of carcinogenesis.
- The value of the parameter p_{sb} is critical for the nanodosimetric conversion model. We assumed a nominal value of 0.15 based on existing radiochemical knowledge and the assumption that the SV is a representative model for cellular DNA. It is important to note that p_{sb} is essentially a radiochemical parameter. Its value depends on the kinetics of the chemical reactions of the initial water radiolysis products (e.g., the hydroxyl radical) within the scavenging environment of the DNA [29]. The subsequent cascade of signaling and repair responses of cells, which is likely to be responsible for the large variations in intrinsic radiosensitivity, should not affect p_{sb}. Therefore, one may assume that the value of p_{sb} is well preserved among different cell types and species.

- The parameter p_{sb} was assumed to be independent of LET. It is possible that the average distance between neighboring ionizations in ionization clusters is smaller for high-LET than for low-LET irradiation. This would mean a higher probability for radicals to recombine before they interact with the DNA and thus a smaller quality factor for high LET than calculated here. We have not yet investigated this effect, but a study of the LET-dependence of the distance between individual ionizations with the Monte Carlo simulation code we have used here will be part of future work.
- Built into the conversion of ionization clusters to strand break clusters is the assumption that a single ion does not produce more than one strand break. This assumption is supported by experimental evidence that low-LET DSBs are formed by two radicals rather than a single radical mechanism and that DSBs produced by alpha particles are formed by several radicals [30].
- It was assumed that only single primary particles contribute to ionization clusters. This assumption is justified by the small geometric cross section of the nanodosimetric SV and the low-dose/fluence space radiation environment [31]. For example, 32 protons of 250 MeV traversing a typical mammalian cell of 20 μm^2 cross section deliver a dose of 0.1 Gy. Based on our estimated absolute cluster size frequency spectrum per unit fluence, we estimate for the probability that more than one out of 32 protons deposit ionization clusters of any size in the 16-nm SV is approximately 10^{-10}, which is negligibly small.

Due to its design, the nanodosimeter in its current implementation does not give any information on the regional association of complex DSBs. The importance of regional spatial clustering of energy deposition events in DNA for the formation of chromosomal exchanges and whether one or two DSBs are needed for these chromosomal rearrangements is still a matter of active debate [32].

Our approach did not predict the sudden decrease of RBE in the high LET range of 100–1000 keV/μm which has been incorporated into the ICRP-defined quality factors. LET-dependent RBE maxima for various biological endpoints, which have served as a database for the choice of quality factors, have been observed over a rather large range of LETs depending on endpoint and particle species [4,26,33]. Other factors than a decrease in the frequency of large clusters may have contributed to the decline of RBE for particles of high LET, for example, the low penetration power of high-LET protons and light ions and saturation effects for heavy ions. Bettega et al. [34] suggested that for low doses of high-LET ions only a fraction of cells are actually traversed by the ions, which would lead to an overkill effect in those cells hit and no effect (except for a possible bystander effect) in those cells not hit. Of note, Groesser et al. [35] investigating the RBE of high-energy iron ions with LETs up to 250 keV/μm for micronucleus formation, which are believed to be the result of complex DSBs, observed leveling-off of RBE for LET values in the 100–250 keV/μm range rather than a peak, similar to the nanodosimetry-defined quality factors reported here.

In recent years, we have obtained experimental nanodosimetric distributions with the nanodosimeter developed at the Weizmann Institute of Science and Loma Linda University with protons of a range of energies and alpha particles [13] as well as high energy electrons from a strontium-90 beta source (unpublished). Such measurements have demonstrated the usefulness of nanodosimetry. However, the current technology has its limitations, foremost its lack of portability due to the need of sophisticated pumping and gas systems and its slow data acquisition time when sampling from a single SV. If the realm of nanodosimetry is to be investigated further, in particular for applications in space radiation protection and monitoring, an improved nanodosimeter is required that can be deployed on spacecraft. For this, the basic concept of the nanodosimetry apparatus may need to be revisited. A compact gas-based nanodosimeter sampling from a large array of SVs would be one possible solution. This will require the development of a two-dimensional ion detector operating in the same low-pressure gas environment as the detection volume. Gas-based two-dimensional micro-pattern detectors exist for photon and electron detection [36] but, so far, not for ions.

In addition, solid-state nanodosimeters of truly nanometer SV size should be investigated and developed in order to further develop this field of research. Attempts to develop solid-state radiation detectors sensitive to the track structure of charged particles was recently undertaken using the response of LiF thermoluminescent detectors (TLD-100) and based on recombination of electron hole pairs in spatially correlated trapping luminescent centers of LiF detectors [37]. It was observed that the shape of the glow peak produced by the TLD depends on the track structure. However, interpretation of this data is complicated and this technology is unsuitable for real-time nanodosimetry. A more effective method for real time nanodosimetry utilizing nanotechnology and quantum dots (QDs) is currently being explored by one of the coauthors (ABR) of this contribution. In contrast to gas nanodosimetry, such a device would register and quantify energy depositions by the track of charged particles in QDs embedded in a tissue-equivalent organic matrix. This mode of solid-state nanodosimetry has the potential for significant improvements over current technology. The development of such detectors would be useful across a range of therapeutic and radiation protection applications, including space radiation; however, an adequate R&D program needs to be conducted.

Conclusions

This study has demonstrated that nanodosimetric data yield meaningful quality factors for space radiation protection, which are based on a biological endpoint namely the ratio of complex DSBs. The advantage of the proposed method is that it does not require identification of individual particles in a complex radiation field. Practical application of nanodosimetry in space radiation protection requires further technical development, in particular, of a compact nanodosimeter as well as biological verification studies.

Acknowledgments

S. S. is supported by the state of Israel, the Ministry of Absorption and the Center for Absorption of Scientists. A. B. is the W. P. Reuther Professor of Research in the peaceful uses of Atomic Energy. A.J.W. was supported by the Australian-American Fulbright Commission.

This work was partially supported by the MINERVA Foundation and the US-Israeli Binational Science Foundation (BSF Grant No. 2002240-1), and by the National Medical Technology Testbed Inc. (NMTB) under the US Department of the Army Medical Research Acquisition Activity, Cooperative Agreement Number DAMD17-97—2-7016. The views, opinions and/or findings contained in this report are those of the authors and should not be construed as a position, policy, decision or endorsement of the Federal Government or the NMTB.

References

[1] Simpson JA. Introduction to the Galactic Cosmic Radiation. In: Shapiro MM, editor. Composition and Origin of Cosmic Rays. New York: Springer; 1983. p. 1–24.
[2] NCRP Report 137. Fluence-based and Microdosimetric Event-based Methods for Protection in Space. Bethesda, MD: National Council on Radiation Protection and Measurements; 2001.
[3] ICRU Report 51. Quantities and Units in Radiation Protection Dosimetry. Bethesda, MD: International Commission on Radiation Units and Measurements; 1993.
[4] ICRP Publication 60. 1990 Recommendations of the International Commission on Radiological Protection. Oxford: Pergamon Press; 1991.
[5] Nikjoo H, Uehara S, Emfietzoglou D, Cucinotta FA. Track-structure Codes in Radiation Research. Radiat Meas 2006;41:1052–74.
[6] Badhwar GD, Atwell W, Badavi FF, Yang TC, Cleghorn TF. Space Radiation Absorbed Dose Distribution in a Human Phantom. Radiat Res 2002;157:76–91.
[7] Curtis SB. Fluence-based and microdosimetric event-based methods for radiation protection in space. J Radiat Res (Tokyo) 2002; 43(Suppl. S):S113–7.
[8] Grosswendt B. Nanodosimetry, from radiation physics to radiation biology. Radiat Prot Dosimetry 2005;115:1–9.
[9] Garty G. Development of ion-counting nanodosimetry and evaluation of its relevance to radiation biology. Ph.D. Thesis, Weizmann Institute of Science, 2004. 〈http://jinst.sissa.it/jinst/theses/2004_JINST_TH_001.jsp〉.
[10] Garty G, Shchemelinin S, Breskin A, Chechik R, Assaf G, Orion I, et al. The performance of a novel ion-counting nanodosimeter. Nucl Instr and Meth Sect A 2002;492:212–35.
[11] Schulte R, Bashkirov V, Shchemelinin S, Breskin A, Chechik R, Garty G, et al. Mapping the sensitive volume of an ion-counting nanodosimeter. J Inst 2006;1:P04004.
[12] Grosswendt B, Pszona S. The track structure of alpha-particles from the point of view of ionization-cluster formation in ''nanometric'' volumes of nitrogen. Radiat Environ Biophys 2002;41:91–102.
[13] Bashkirov V, Schulte R, Breskin A, Chechik R, Schemelinin S, Garty G, et al. Ion-counting nanodosimeter with particle tracking capabilities. Radiat Prot Dosim 2006;122:415–9.
[14] Wroe A, Schulte R, Bashkirov V, Rosenfeld AB, Keeney B, Spradlin P, et al. Nanodosimetric cluster size distributions of therapeutic proton beams. IEEE Trans Nucl Sci 2006;53:532–8.
[15] Hilgers G, Gargioni E, Grosswendt B, Shchemelinin S. Proton-induced frequency distribution of ionization cluster size in propane. Radiat Prot Dosimetry 2007 Jun 1; [Epub ahead of print].
[16] J. F. Ziegler and J.P. Biersack, SRIM. http://www.srim.org/#SRIM, 2003.
[17] Garty G, Schulte R, Shchemelinin S, Grosswendt B, Leloup C, Assaf G, et al. First attempts at prediction of DNA strand-break yields using nanodosimetric data. Radiat Prot Dosimetry 2006; 122:451–4.
[18] Milligan JR, Aguilera JA, Ward JF. Variation of single-strand break yield with scavenger concentration for plasmid DNA irradiated in aqueous solution. Radiat Res 1993;133:151–7.
[19] Paganetti H, Niemierko A, Ancukiewicz M, Gerweck LE, Goitein M, Loeffler JS, et al. Relative biological effectiveness (RBE) values for proton beam therapy. Int J Radiat Oncol Biol Phys 2002;53: 407–21.
[20] Goodhead DT, Belli M, Mill AJ, Bance DA, Allen LA, Hall SC, et al. Direct comparison between protons and alpha-particles of the same LET: I. Irradiation methods and inactivation of asynchronous V79, HeLa and C3H 10T1/2 cells. Int J Radiat Biol 1992;61:611–24.
[21] Belli M, Goodhead DT, Ianzini F, Simone G, Tabocchini MA. Direct comparison of biological effectiveness of protons and alpha-particles of the same LET. II. Mutation induction at the HPRT locus in V79 cells. Int J Radiat Biol 1992;61:625–9.
[22] Wroe AJ, Cornelius IM, Rosenfeld AB, Pisacane VL, Ziegler JF, Nelson ME, et al. Microdosimetry simulations of solar protons within a spacecraft. IEEE Trans Nucl Sci 2005;52:2591–6.
[23] Pisacane VL, Ziegler JF, Nelson ME, Caylor M, Flake D, Heyen L, et al. MIDN: a spacecraft microdosimeter mission. Radiat Prot Dosimetry 2006;120:421–6.
[24] ICRU Report 36. Microdosimetry. Bethesda, MD: International Commission on Radiation Units and Measurements; 1983.
[25] National Research Council (NRC) Health Risks from Exposure to Low Levels of Ionizing Radiation (BEIR VII-phase 2). Washington DC: The National Academic Press; 2006.
[26] ICRP Publication 92. Relative Biological Effectiveness (RBE), Quality Factor (Q), and Radiation Weighting Factor (w_R). Oxford, UK: Elsevier Science Ltd.; 2003.
[27] Prise KM, Ahnström G, Belli M, Carlsson J, Frankenberg D, Kiefer J, et al. A review of dsb induction data for varying quality radiations. Int J Radiat Biol 1998;74:173–84.
[28] Iliakis G, Wang H, Perrault AR, Boecker W, Rosidi B, Windhofer F, et al. Mechanisms of DNA double strand break repair and chromosome aberration formation. Cytogenet Genome Res 2004;104:14–20.
[29] Ly A, Aguilera JA, Milligan JR. Kinetic behavior of the reaction between hydroxyl radical and the SV40 minichromosome. Radiat Phys Chem 2007;76:982–7.
[30] Pfeiffer P, Göttlich B, Reichenberger S, Feldmann E, Daza P, Ward JF, et al. DNA lesions and repair. Mutat Res 1996;366:69–80.
[31] Alpen EL, Powers-Risius P, Curtis SB, DeGuzman R, Fry RJ. Fluence-based relative biological effectiveness for charged particle

carcinogenesis in mouse Harderian gland. Adv Space Res 1994;14: 573–81.
[32] Cornforth MN. Perspectives on the formation of radiation-induced exchange aberrations. DNA Repair (Amst) 2006;5:1182–91.
[33] NCRP Report 104. The Relative Biological Effectiveness of Radiations of Different Quality. Bethesda, MD: National Council on Radiation Protection and Measurements; 1990.
[34] Bettega D, Calzolari P, Doneda L, Durante M, Tallone L. Early and delayed reproductive death in human cells exposed to high energy iron ion beams. Adv Space Res 2005;35:280–5.
[35] Groesser T, Chun E, Rydberg B. Relative biological effectiveness of high-energy iron ions for micronucleus formation at low doses. Radiat Res 2007;168:675–82.
[36] Maia JM, Mrmann D, Breskin A, Chechik R, Veloso JFCA, dos Santos JMF. 2-D imaging with cascaded GEM/MHSP multipliers. JINST 2007;2:P09008.
[37] Horowitz YS, Satinger D, Avila O. Track structure approach to the calculation of peak 5a to peak 5 (TLD-100) relative intensities following heavy charged particle irradiation. Radiat Prot Dosimetry 2006;119:45–8.

Available online at www.sciencedirect.com
ScienceDirect